

circ_0067934 promotes the progression of papillary thyroid carcinoma cells through miR-1301-3p/HMGB1 axis

Liang-Peng DONG¹, Ling-Yun CHEN², Bin BAI¹, Xiao-Fen QI¹, Jing-Nan LIU¹, Shuang QIN^{1,*}

¹Department of Thyroid Breast Surgery, The First Affiliated Hospital of Xinxiang Medical University, Weihui, Henan, China; ²Department of Operating Room, The First Affiliated Hospital of Xinxiang Medical University, Weihui, Henan, China

*Correspondence: qinshuang19879@163.com

Received June 8, 2021 / Accepted July 28, 2021

Papillary thyroid carcinoma (PTC) is the most prevalent form of thyroid cancer (TC). There is increasing evidence that circular RNAs play a role in the tumorigenesis of PTC. The aim of our study was to evaluate the potential function of circ_0067934 in PTC and the underlying molecular mechanism. In our study, cell viability assay, quantitative real-time PCR (qRT-PCR), colony formation assay, flow cytometry, wound-healing assay, Transwell invasion assay, western blot, soft agar assay, RNA immunoprecipitation (RIP), dual-luciferase reporter assay, immunohistochemical (IHC) staining, and tumor xenograft formation were conducted to evaluate the effects of circ_0067934 in PTC cells. We found that circ_0067934 was upregulated in PTC tissues and cell lines. Knockdown of circ_0067934 inhibited growth, colony formation, migration, invasion, EMT, and tumor xenograft growth, and induced apoptosis of PTC cells. Moreover, circ_0067934 acted as a molecular sponge for miR-1301-3p, and depletion of miR-1301-3p abrogated the effects of circ_0067934 knockdown in PTC cells. In addition, HMGB1 was a target of miR-1301-3p, and miR-1301-3p overexpression inhibited the malignant effects of PTC cells via suppressing HMGB1. Furthermore, knockdown of circ_0067934 suppressed HMGB1 expression, PI3K/Akt, and MAPK activation by sponging miR-1301-3p. In nude mice, circ_0067934 depletion repressed tumor xenograft growth of PTC cells. In conclusion, our results provided a novel insight into circ_0067934 in the tumorigenesis and progression of PTC. circ_0067934 might be a prognostic marker or therapeutic target for PTC treatment.

Key words: circ_0067934, miR-1301-3p, HMGB1, thyroid cancer

Thyroid carcinoma (TC) is the most common endocrine-associated cancer worldwide, which accounts for about 2.9% of all cancers [1]. Papillary thyroid carcinoma (PTC) is the main histological subtype for TC, taking up more than 80% of all cases [2]. The global incidence rate of PTC in adults is increasing year by year, from 7.9/100,000 in 2000 to 16.9/100,000 in 2017 [3]. PTC is curable or controllable in most patients under current treatment options, such as thyroid hormone suppression, surgical resection, and oral iodine treatment. However, just as most other cancers, a small proportion of PTC patients have a poor prognosis. These patients have certain clinicopathological features, such as large primary tumors, lymph node metastasis, and distant metastasis [4, 5]. The development of novel strategies may be important for treating these patients. For example, the development of new plant extracts to inhibit cancer [6], combining therapy to enhance chemosensitivity [7, 8] and radiosensitivity [9], development of novel strategy for drug delivery [10], and oncogene targeted therapies [11, 12] are

all promising strategies for solid cancer treatment. Similarly, it is of great significance to study novel therapeutic targets for PTC.

In recent years, non-coding RNAs attract much more attention for their potential roles in tumor initiation and progression of cancers [13–18]. Circular RNAs (circRNAs), which are mainly transcribed from the intergenic region of the genome, have drawn much attention for cancer transcriptome research. The cancer-promoting or inhibiting roles of circRNAs have been well characterized [19]. For example, circRNA_102171 is reported to facilitate the progression of PTC by regulating the Wnt/ β -catenin activation [20]. In another study, circ_0058124 is proved to promote tumorigenesis and invasiveness of PTC through the NOTCH3/GATAD2A signaling axis [21]. circ_0067934 is circRNA derived from the human protein kinase Ciota (PRKCI) gene locus at chromosome 3q26.2 [22]. Previous studies indicate that circ_0067934 plays a role in tumorigenesis of many cancers, such as hepatocellular carcinoma [23], esophageal

squamous cell carcinoma [24], and cervical cancer [25]. More importantly, circ_0067934 is reported to upregulate and correlates with poor prognosis of TC [26]. Though a previous report indicates that circ_0067934 promotes TC progression by regulating the miR-1304/CXCR1 axis [22], we speculate that circ_0067934 may have other uncharacterized targets or effects in PTC.

MicroRNAs are non-coding RNAs of 18–25 nucleotides in length. They can regulate gene expression at post-transcriptional levels, thus playing a role in tumorigenesis. For example, miR-203 regulates the growth and stemness of estrogen receptor-positive breast cancer cells by suppressing SOCS3 expression [27]. LncRNA MIR22HG, the host gene of microRNAs miR-22-3p and miR-22-5p, promotes growth and invasion of glioblastoma cells by inhibiting the Wnt/ β -catenin signaling pathway through the loss of miR-22-3p and miR-22-5p [28]. There are increasing evidences that circRNAs regulate multiple cellular functions by acting as a molecular sponge for microRNAs. For instance, circRNA cRAPGEF5 inhibits proliferation and migration of renal cell carcinoma cells by sponging miR-27a-3p and subsequently increasing TXNIP expression [29]. circFOXM1 is upregulated in PTC cells and promotes tumor growth by sponging miR-1179 [30]. Moreover, circ_0067934 is reported to act as a molecular sponge for microRNAs in hepatocellular carcinoma [23], cervical cancer [25], and lung cancer [31].

In this study, the potential functions of circ_0067934 in PTC were explored. The proliferation, apoptosis, migration, invasion, and tumor formation of PTC cells were evaluated after circ_0067934 knockdown. Our data provided a novel insight of circ_0067934 in the progression of PTC. We showed that circ_0067934 acted as a molecular sponge for miR-1301-3p, thus increasing the level of HMGB1 and facilitating the development of PTC.

Materials and methods

Collection of clinical tissue specimens. A total of 30 papillary thyroid carcinoma specimens and paired normal tissues were collected from the First Affiliated Hospital of Xinxiang Medical University from May 2015 to March 2019. The clinical pathological features were diagnosed by two pathologists independently. The use of clinical samples in this study was approved by the Institute Research Ethics Committee of the First Affiliated Hospital of Xinxiang Medical University and written consents were obtained from all enrolled patients. The tissue specimens were cut into small blocks, snapped frozen in liquid nitrogen, and stored at -80°C for further use. The demographic and clinicopathological features of enrolled patients were extracted from the hospital database.

Cell culture and transfection. The HEK293, Nthy-ori3-1 normal thyroid cell line, and PTC cell lines (TPC-1, SW579, FTC133, MDA-T32, MDA-T120, and XTC-1) were purchased from the American Type Culture Collection (ATCC). PTC

cell line KAT-5 was purchased from the Chinese Academy of Sciences (Shanghai, China). All cells were cultured in Dulbecco's Modified Eagle's Medium (DMEM, Gibco, Carlsbad, CA, USA) containing 10% fetal bovine serum (FBS, Gibco), 0.5% penicillin, and 0.5% streptomycin in a humidified incubator at 37°C with 5% CO_2 . The mycoplasmas were tested every 4 weeks to rule out mycoplasma contamination in cultured cells. All cells were verified by STR methods in our study. Cell transfection was carried out using Lipofectamine 3000 (Invitrogen, USA) as protocol indicated. The transfection efficacy was certified to reach at least 60% for all experiments.

Plasmid constructs. Small interfering RNA (si-RNA) for circ_0067934 (5'-UGUUG AUUGG GAUUAU GUUAUU-3') were obtained from RiboBio (China). The sequences for si-NC were 5'-GAAUG CUCCG UAAUC UGAACC-3'. circ_0067934 expression plasmid, miR-1301-3p mimics, anti-miR-1301-3p, and controls were obtained from RiboBio (China). HMGB1 coding sequence was inserted into the pcDNA3 vector (Invitrogen, Thermo Fisher Scientific, Inc.) for HMGB1 overexpression. Small hairpin RNA for circ_0067934 was constructed by cloning the targeting sequence into pLKO.1 plasmid. The sh-RNA sequence for circ_0067934 was: 5'-TTGTG TATGT GTAAA TAATA TAT-3'. Empty pLKO.1 plasmid was used as sh-NC.

RNA extraction and quantitative real-time PCR (qRT-PCR). Total RNAs from tissues and cell lines were extracted by TRIzol reagent (Invitrogen, CA, USA) as protocol indicated. RNase R was used to degrade poly(A) tailed linear RNA. M-MLV Reverse Transcriptase (Invitrogen) and miScript Reverse Transcription Kit (QIAGEN, Hilden, Germany) were used to synthesize the complementary DNA (cDNA). All-in-one miRNA RT-qPCR Detection Kit (GeneCopoeia, Guangzhou, China) or QuantiTect SYBR Green PCR Kit (Qiagen) was used for in qRT-PCR. The amplification reactions were: 94°C 10 min, 29 cycles of 94°C 30 s, 55°C 30 s, and 72°C 30 s. GAPDH was used as an internal control. The relative RNA levels were calculated by the Cq method. The primers used were: circ_0067934, forward: 5'-TAGC AGTT CCCC AATC CTTG-3'; reverse: 5'-CACA AATT CCCA TCAT TCCC-3'; miR-1301-3p, forward: 5'-TTAC AGCT GCCT GAGA GTGA CTTA-3'; reverse: 5'-CTCT ACAG CTAT ATTG CCAG CCA-3'; HMGB1 forward: 5'-TTTC AAAC AAAG ATGC CACA-3'; reverse: 5'-GTTC CCTA AACT CCTA AGCA GATA-3'; U6, forward: 5'-GCAG ACCG TTCG TCAA CCTA-3'; reverse: 5'-AATT CTGT TTGC GGTG CGTC-3'; GAPDH, forward: 5'-GAAG GTGA AGGT CGGA GTC-3'; reverse: 5'-GAAG ATGG TGAT GGGG TTTC-3'. Each sample was done in triplicates.

RNA immunoprecipitation (RIP). RIP was conducted using the BersinBio™ RNA Immunoprecipitation Kit (BersinBio, Guangzhou, China) according to the manufacturer's instructions. Briefly, cell lysates were incubated with beads for 16 h at 4°C , then washed with RIP wash buffer 5 times. Then, beads were incubated with anti-Ago2 (Cell

Signaling #2897, 1:200, USA) or anti-IgG (Abcam #ab238004, 1:300, USA) for 16 h at 4°C. The pulled-down RNA was evaluated by qRT-PCR. All assays were done in triplicates.

Cell viability assay. The viability of cells was tested using the CCK-8 assays. In brief, TPC-1 and SW579 cells were seeded in 96-well plates at a density of 3,000 cells/well. At each time point, a CCK-8 reagent (10 μ l) was added to each well and the cells were incubated at 37°C for 4 h. The absorbance at 450 nm was measured by a microplate reader. Each sample was done in triplicates.

Colony formation assay. Cells (500/well) were seeded in 6-well plates for 2 weeks without disturbance. Then, cells were fixed by 4% paraformaldehyde for 10 min at room temperature. Cells were washed with PBS 2 times and stained with 0.1% crystal violet for 60 min at room temperature. The image of colonies was obtained by a scanner. Each sample was done in triplicates.

Soft agar assay. A soft agar assay was conducted as previously reported [32]. Briefly, cells (5000/well) were seeded in 0.4% top agar for three weeks. Then, colonies were stained with 0.5 mg/ml thiazolyl blue tetrazolium bromide (MTT, Sigma-Aldrich, USA) at 37°C for 3 h. The image of colonies was obtained by a scanner. Each sample was done in triplicates.

Flow cytometry. Cells apoptosis was measured by flow cytometry. In brief, cells were digested with 0.5% trypsin, washed with cold PBS three times, and resuspended in the binding buffer. Then, cells (1×10^6) were incubated with 5 μ l Annexin FITC and 10 μ l PI (Beyotime, Jiangsu, China) at 4°C for 30 min. Fluorescent signals at 488/530 were analyzed by Gallios Flow Cytometer (Beckman Coulter). Each sample was done in triplicates.

Wound-healing assay. Cell migration of TPC-1 and SW579 cells was evaluated by wound-healing assay. After the cell confluence reached 90%, a straight scratch in the middle of the well was created by a sterile pipette tip. Cell debris was washed away by PBS 3 times. Then, cells were cultured for another 24 h. Images were taken at 0 h and 24 h after scratching. The migration distance was analyzed using the ImageJ software. Three replicate wells were performed for each group.

Transwell invasion assay. Transwell chamber (Costar Corp, USA) was pre-coated with Matrigel (BD Biosciences, USA). TPC-1 or SW579 cells (1×10^5) were seeded in the upper chamber without serum. Then, a normal culture medium with 10% FBS (500 μ l) was added into the lower chamber. The invasion cells at 48 h later were fixed by methanol (Solarbio) for 15 min at room temperature, stained with 0.1% crystal violet (Solarbio) for 1 h at room temperature, and photographed under a microscope (Olympus). Ten fields of invasion cells were randomly chosen under the microscope, and three of them were chosen as representative images. Each sample was done in triplicates.

Western blot analysis. Cell lysates were extracted by RIPA lysis buffer (Beyotime, China) with protease inhibi-

tors (Sigma, USA). Protein concentration was determined by the BCA kit (Beyotime, China). A total of 25 μ g protein was separated by 10% or 15% SDS-PAGE, then transferred onto polyvinylidene fluoride (PVDF) membranes (Millipore, Massachusetts, USA). The membranes were blocked by 5% non-fat milk for 1 h at room temperature, incubated with the primary antibodies at 4°C overnight, and corresponding secondary antibodies for 1 h at room temperature. The following antibodies were used: anti-E-cadherin (ab76055, 1:1000), anti-Vimentin (ab92547, 1:1000), anti-HMGB1 (ab79823, 1:1000), anti-Cleaved Caspase-3 (ab32042, 1:1000), anti-Cleaved PARP (ab32064, 1:1000), anti-p-PI3K (ab278545, 1:1000), anti-PI3K (ab32089, 1:1000), anti-p-AKT (ab8805, 1:1000), anti-AKT (phospho T308) (ab38449, 1:1000), anti-MAPK (ab184699, 1:1000), anti-p-MAPK (ab201015, 1:1000), and anti-GAPDH (ab8245, 1:1000) were purchased from Abcam, USA. A ChemiDoc XRS imaging system and Quantity One analysis software (Bio-Rad, San Francisco, CA, USA) were used for detecting and analyzing the expression of indicated proteins. GAPDH was used as an endogenous control. All assays were repeated three times.

Dual-luciferase reporter assay. The potential binding sites between circ_0067934 and mir_1301-3p, or HMGB1 and miR-1301-3p, were predicted by starBase 2.0 or Target Scan 7.2. The 3'-UTR of HMGB1 or circRNA_0067934 fragments with targeted binding sites were inserted into pMIR-REPORT vectors. Mutated plasmid generated by Quickchange site-directed mutagenesis kit (Agilent Technologies, USA). Cells were co-transfected with pMIR-REPORT vectors containing 3'-UTR of HMGB1 or circRNA_0067934 fragments with targeted binding sites, miR-1301-3p mimics or miR-NC, and a Renilla luciferase plasmid (2:2:1). The Dual-Luciferase reporter assay system (Promega, USA) was used for measuring luciferase activity. Each sample was done in triplicates.

Tumor xenograft assay. The animal experiments were performed in strict accordance with the protocol approved by the Institutional Committee for Animal Research of the First Affiliated Hospital of Xinxiang Medical University. BALB/C nude mice (male, 4-week-old, n=5/group) were purchased from the Kunming Research Center of Laboratory Animal. After accustomed for one week, the mice were subcutaneously injected with 4×10^6 cells (TPC-1 cells stably transfected with sh-circ_0067934 or sh-control). One week later, tumor volume was measured every 4 days by caliper. Mice were anesthetized with 4% isoflurane and sacrificed by cervical dislocation at the end of the experiments. Tumors were dissected out and weighed. Tumor volume was calculated by the formula: (length \times width²)/2.

TUNEL assay. Apoptosis of TPC-1 and SW579 cells was detected by TUNEL fluorescence FITC kit (Roche, USA) according to the manufacturer's instructions. In brief, sections were deparaffinized by xylene and rehydrated by alcohol gradients. After digesting with 20 μ g protease K at 37°C for 30 min, the sections were incubated with TUNEL

staining buffer at 37°C for 1 h avoiding light. DAPI (Thermo Fisher Scientific, Waltham, MA, USA) was used to stain the nuclei for 15 min at room temperature. Images were taken by a laser scanning confocal microscope (Olympus, Fluoview1000, Tokyo, Japan).

Immunohistochemical (IHC) staining. Tumors were fixed by 4% PFA overnight, embedded in paraffin, and sliced at 5 μ m thickness. Next, sections were deparaffinized by xylene, rehydrated by alcohol gradients, and microwave-heated in pH 6.0 citrate buffer for the antigen retrieval. The slices were then blocked with 1% BSA for 1 h at room temperature, incubated with primary antibody against HMGB1 (Abcam #ab79823, 1:300), E-Cadherin (Abcam #ab212059, 1:300), or Vimentin (Abcam #ab92547, 1:300) at 4°C overnight, and corresponding HRP-conjugated secondary antibodies for 1 h at room temperature. The DAB substrates were then added and sections were observed under a laser scanning confocal microscope (Olympus, Fluoview1000, Tokyo, Japan).

Statistical analysis. SPSS statistical software (version 20.0, SPSS Inc., USA) was used for statistical analysis. Data are shown as mean \pm SD. Student's t-test or one-way ANOVA (two-sided) was used for comparison between two or more groups. A p-value \leq 0.05 was considered statistically significant.

Results

circ_00067934 is upregulated in papillary thyroid carcinoma tissues and cell lines. The expression of circ_00067934 in PTC tissues and paired adjacent normal tissues was evaluated by RT-qPCR. We found that circ_00067934 was upregulated in thyroid cancer tissues compared with adjacent normal tissues (Figure 1A). These patients were divided into circ_00067934 high expression group and low expression group by using the median expression as a cut-off value. We found that high expression of circ_00067934 was positively correlated with larger tumor size, advanced tumor stage, and lymph node metastasis (Table 1). Meanwhile, the expression of circ_00067934 in PTC cell lines and normal thyroid cell

Nthy-ori3-1 was tested, too. Compared with Nthy-ori3-1, circ_00067934 was upregulated in TPC-1, SW579, FTC113, MDA-T32, and KAT-5 cells (Figure 1B). Taken together, we found that circ_00067934 was upregulated in papillary thyroid carcinoma tissues and cell lines.

Knockdown of circ_00067934 restrains growth, migration and invasion, and induces apoptosis of PTC cells.

To explore the potential function of circ_00067934 in PTC cells, we knocked down its expression by siRNA specifically targeting circ_00067934. RT-qPCR results confirmed that we successfully knocked down circ_00067934 in TPC-1 and SW579 cells (Figure 2A). TPC-1 and SW579 cells were chosen for loss-of-function studies for their high expression of circ_00067934 compared with other PTC cell lines. In cell viability assay and colony formation assay, knockdown of

Table 1. Correlation between circ_00067934 expression and clinicopathological characteristics in papillary thyroid carcinoma patients.

Characteristics	n	circ_00067934 expression		p-value
		Low	High	
Age (Years)				0.856
\leq 60	11	5	6	
$>$ 60	19	9	10	
Sex				0.905
Male	12	7	5	
Female	18	7	11	
Tumor size (mm)				0.041
\geq 30	19	6	13	
$<$ 30	11	8	3	
Tumor stage				0.018
T1+T2	8	6	2	
T3+T4	22	8	14	
Lymphatic metastasis				0.001
Positive	19	5	14	
Negative	11	9	2	
Distant metastasis				0.143
Positive	12	4	8	
Negative	18	10	8	

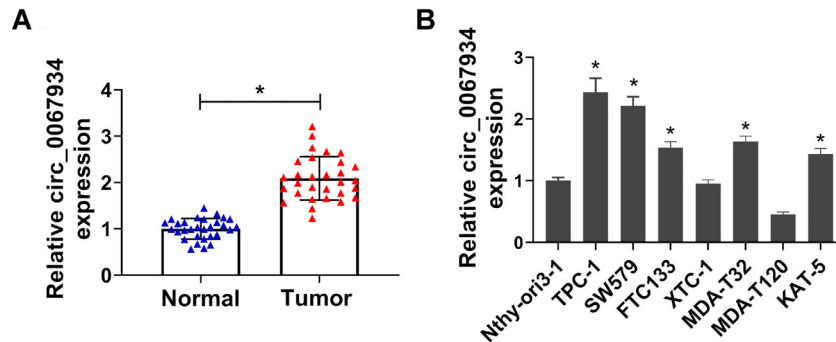


Figure 1. circ_00067934 is upregulated in papillary thyroid carcinoma tissues and cell lines. (A) circ_00067934 expression in 30 TC tissues compared with adjacent normal tissues was detected by qRT-PCR. (B) circ_00067934 expression in PTC cell lines and normal thyroid cell line Nthy-ori3-1 was evaluated by RT-PCR. *p<0.05. Each sample was done in triplicate.

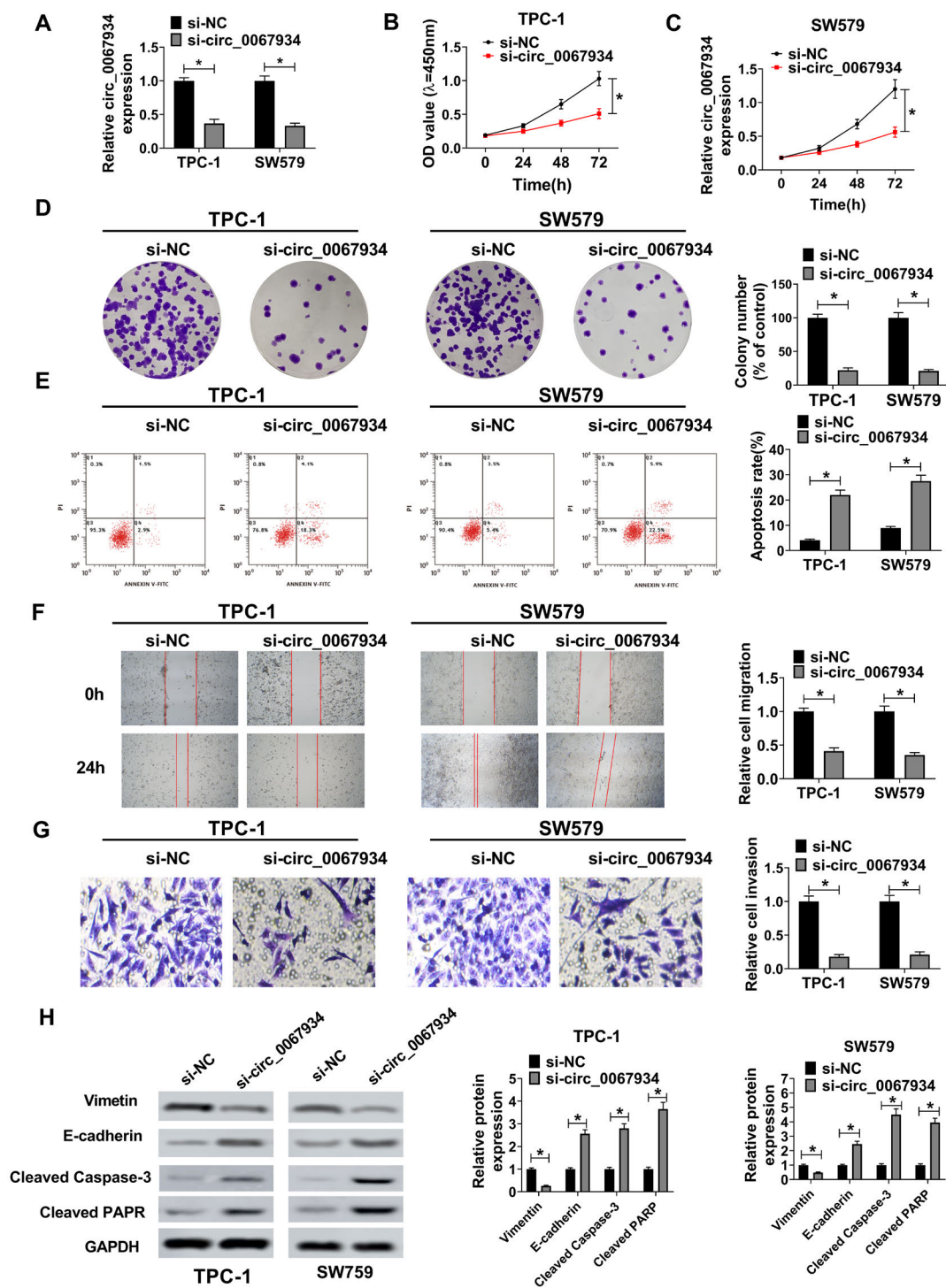


Figure 2. Knockdown of circ_00067934 restrains growth, migration and invasion, and induces apoptosis of PTC cells. (A) TPC-1 and SW579 cells were transfected with si-circ_00067934 or si-NC, then relative circ_00067934 expression was evaluated by qRT-PCR. (B and C) TPC-1 and SW579 cells transfected with si-circ_00067934 or si-NC were seeded in 96-well plates (3000 cells/well), then cell viability at 0, 24, 48, and 72 h was evaluated. (D) TPC-1 and SW579 cells transfected with si-circ_00067934 or si-NC were seeded in 6-well plates (500 cells/well) for colony formation assay. Representative plates and colony numbers were shown. (E) TPC-1 and SW579 cells transfected with si-circ_00067934 or si-NC were used for flow cytometry analysis. (F) TPC-1 and SW579 cells transfected with si-circ_00067934 or si-NC were used for the wound-healing assay. Representative images and relative migration distance were shown. (G) TPC-1 and SW579 cells transfected with si-circ_00067934 or si-NC were used for Transwell invasion assay. Representative images and relative invasion cells were shown. (H) TPC-1 and SW579 cells transfected with si-circ_00067934 or si-NC were used for western blot. * $p < 0.05$. Each sample was done in triplicate.

circ_00067934 suppressed growth and colony formation of TPC-1 and SW579 cells (Figure 2B–2D). In flow cytometry analysis, knockdown of circ_00067934 induced apoptosis of TPC-1 and SW579 cells (Figure 2E). However, we did not find any difference in the cell cycle of TPC-1 and SW579 cells after circ_00067934 knockdown (Supplementary Figure S1A). Cyclin E and p21 are makers for cell cycle progression. There was no significant difference in the expression of Cyclin E and p21 after circ_00067934 knockdown, too (Supplementary Figure S1B). The migration and invasion of PTC cells were evaluated by wound-healing assay and Transwell invasion assay. We found that knockdown of circ_00067934 restrained migration and invasion of TPC-1 and SW579 cells (Figures 2F, 2G). The expression of epithelial-mesenchymal transition (EMT) markers E-cadherin and Vimentin was evaluated by western blot. We found that silencing

circ_00067934 suppressed the expression of Vimentin and increased the expression of E-cadherin, indicating that knockdown of circ_00067934 suppressed EMT (Figure 2H). In addition, we found that circ_00067934 overexpression promoted anchorage-independent growth of normal thyroid cell Nthy-ori3-1, indicating that circ_00067934 facilitated the malignant transformation of PTC cells (Supplementary Figure S2). Collectively, our results indicated that knockdown of circ_00067934 restrained growth, migration and invasion, and induced apoptosis of PTC cells.

miR-1301-3p was a direct target of circ_00067934 in PTC cells. The potential miRNAs that interacted with circ_00067934 were predicted by starBase 2.0 or Target Scan 7.2. miR-1301-3p was finally selected in our study and the predicted binding sites of circ_00067934 and miR-1301-3p are shown in Figure 3A. The interaction between circ_00067934

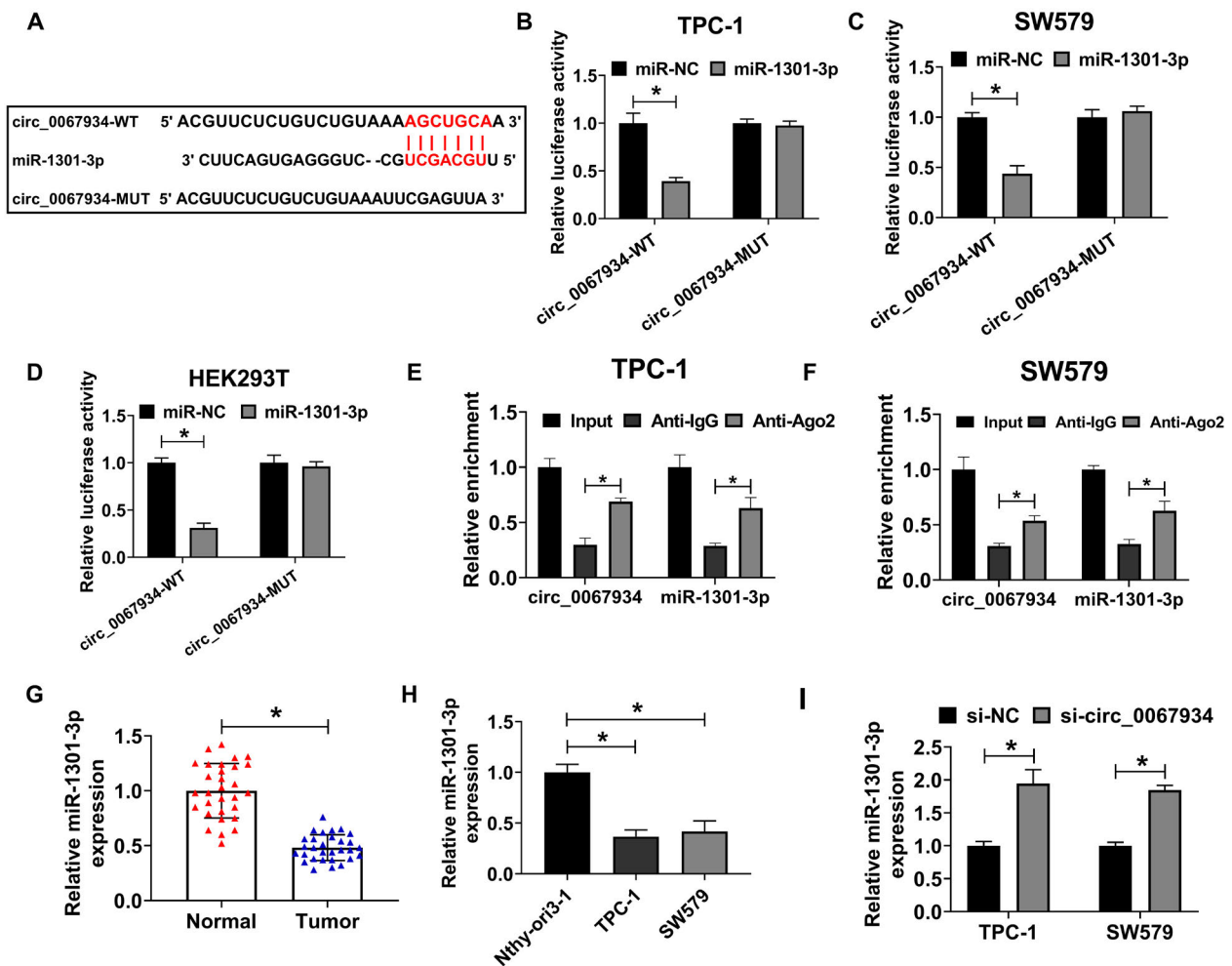


Figure 3. miR-1301-3p was a direct target of circ_00067934 in PTC cells. (A) The predicted binding sites of circ_00067934 and miR-1301-3p. (B–D) TPC-1, SW579, or HEK293T cells were co-transfected with circ_00067934 WT or MUT, miR-1301-3p, or miR-NC for luciferase reporter assay. (E and F) Lysates from TPC-1 and SW579 cells were collected for RIP assay. Relative circ_00067934 and miR-1301-3p levels are shown. (G) miR-1301-3p expression in PTC tissues and adjacent normal tissues was tested by qRT-PCR. (H) miR-1301-3p expression in PTC cell lines was tested by qRT-PCR. (I) TPC-1 and SW579 cells were transfected with si-circ_00067934 or si-NC, then the expression of miR-1301-3p was tested by qRT-PCR. * $p < 0.05$. Each sample was done in triplicate.

and miR-1301-3p was further verified by the dual-luciferase report assay. We found that overexpression of miR-1301-3p could remarkably reduce the luciferase activity of wild type circ_00067934 (WT) but this was abrogated in circ_00067934 with 2 bp mutations at the predicted binding sites (MUT) (Figures 3B–3D). The interaction between circ_00067934 and miR-1301-3p was further validated by the RIP assay. We found that circ_00067934 and miR-1301-3p were simultaneously pulled down by Anti-Ago2 in TPC-1 and SW579 cells (Figures 3E, 3F). The expression levels of miR-1301-3p in PTC tissues and cell lines were evaluated by RT-qPCR. Notably, miR-1301-3p was downregulated in PTC tissues compared with paired normal tissues (Figure 3G). Besides, a decreased expression of miR-1301-3p was observed in TPC-1 and SW579 cells compared with Nthy-ori3-1 cells (Figure 3H). Moreover, silencing of circ_00067934 increased the expression of miR-1301-3p in both TPC-1 and SW579 cells (Figure 3H). Above all, our results indicated that miR-1301-3p was a direct target of circ_00067934 in PTC cells.

Depletion of miR-1301-3p suppresses the effects of circ_00067934 knockdown in PTC cells. To explore whether miR-1301-3p was critical for the function of circ_00067934 in PTC cells, we depleted miR-1301-3p in PTC cells by anti-miR-1301-3p. As showed in Figure 4A, knockdown of circ_00067934 increased the levels of miR-1301-3p in both TPC-1 and SW579 cells, and this was reversed by anti-miR-1301-3p. Moreover, the inhibitory effects of si-circ_00067934 on the cell growth and colony formation of TPC-1 and SW579 cells were overturned by the co-transfection of anti-miR-1301-3p (Figures 4B–4D). Besides, knockdown of circ_00067934 promoted apoptosis of TPC-1 and SW579 cells, but this was abrogated by adding anti-miR-1301-3p (Figure 4E). In wound scratch healing assay and Transwell invasion assay, anti-miR-1301-3p reversed the inhibitory effects of si-circ_00067934 on migration and invasion of TPC-1 and SW579 cells, too (Figures 4F, 4G). In western blot analysis, si-circ_00067934 decreased Vimentin and increased E-cadherin expression, but this was reverted by anti-miR-1301-3p (Figures 4H, 4I). Taken together, our results indicated that depletion of miR-1301-3p suppressed the effects of circ_00067934 knock down in PTC cells.

HMGB1 is a target of miR-1301-3p in PTC cells. The downstream target of miR-1301-3p in PTC cells was predicted by starBase 2.0 or Target Scan 7.2. We found that HMGB1 was predicted to be targeted by miR-1301-3p (Figure 5A). In dual-luciferase reporter assay, co-transfection of miR-1301-3p reduced the luciferase activity of WT HMGB1 but this was abolished in MUT HMGB1, indicating that HMGB1 was targeted by miR-1301-3p in PTC cells (Figures 5B, 5C). Moreover, HMGB1 was upregulated in PTC tissues compared with paired normal tissues (Figure 5D–5F). Meanwhile, the levels of HMGB1 were higher in TPC-1 and SW579 cells than that in Nthy-ori3-1 cells (Figures 5G, 5H). Furthermore, miR-1301-3p mimics suppressed the expression of HMGB1 in TPC-1 and SW579 thyroid cancer cells

(Figures 5I, 5J). Collectively, our data indicate that HMGB1 was a target of miR-1301-3p in PTC cells.

miR-1301-3p inhibits the malignant potential of PTC cells via suppressing HMGB1. To validate whether HMGB1 was involved in the antitumor effect of miR-1301-3p, HMGB1 was overexpressed in miR-1301-3p transfected PTC cells. Overexpression of HMGB1 in our study abolished the inhibition of miR-1301-3p on HMGB1 levels in TPC-1 and SW579 cells (Figures 6A, 6B). Moreover, transfection of miR-1301-3p mimics caused significant inhibition on the viability, colony formation, migration and invasion, and increasing of apoptosis in TPC-1 and SW579 cells but all these effects were reversed by co-transfection with HMGB1 (Figures 6C–6H). In addition, miR-1301-3p reduced the protein levels of vimentin and increased the protein levels of E-cadherin, but this was abrogated by HMGB1 overexpression in TPC-1 and SW579 cells (Figures 6I, 6J). Above all, these results suggested that miR-1301-3p inhibited the malignant potential of PTC cells via suppressing HMGB1.

Knockdown of circ_0067934 suppressed HMGB1 expression, PI3K/Akt, and MAPK activation through sponging miR-1301-3p. Accumulated studies indicate that HMGB1 is involved in the PI3K/Akt and MAPK signaling in cancer cells [33–35], thus we speculated that circ_0067934 might regulate PI3K/Akt and MAPK signaling through the miR-1301-3p/HMGB1 axis. We found that knockdown of circ_0067934 inhibited HMGB1 expression in TPC-1 and SW579 cells but this was reverted by anti-miR-1301-3p (Figures 7A, 7B). Moreover, we found that knockdown of circ_0067934 suppressed the phosphorylation of PI3K, Akt, and MAPK but this was partially abrogated by anti-miR-1301-3p (Figures 7A, 7B). The correlation of circ_0067934, miR-1301-3p, and HMGB1 expression in PTC patients was explored by Pearson correlation analysis. Our data indicated that circ_0067934 expression was negatively correlated with miR-1301-3p but positively associated with HMGB1 in PTC patients (Figures 7C–7E).

circ_0067934 depletion repressed tumor xenograft growth of PTC cells. Finally, *in vivo* tumorigenesis of PTC cells was applied to further validate the critical role of circ_0067934 in thyroid cancer. In our study, TPC-1 cells stably transfected with sh-circ_0067934 or sh-NC were subcutaneously injected into the nude mice. As illustrated in Figures 8A and 8B, knockdown of circ_0067934 impaired tumor xenograft growth of TPC-1 cells. The levels of circ_0067934, miR-1301-3p, and HMGB1 were tested in tumor xenografts. As indicated in Figures 8C–8F, the levels of circ_0067934 and HMGB1 were reduced in the sh-circ_0067934 group compared with that in the sh-NC group. In TUNEL staining, the apoptosis of transfected cells was increased by the knockdown of circ_0067934 (Figure 8G). Furthermore, IHC staining showed an increased expression of E-cadherin and decreased expression of HMGB1 and Vimentin after circ_0067934 knockdown (Figure 8H). Finally, a schematic diagram was drawn to show

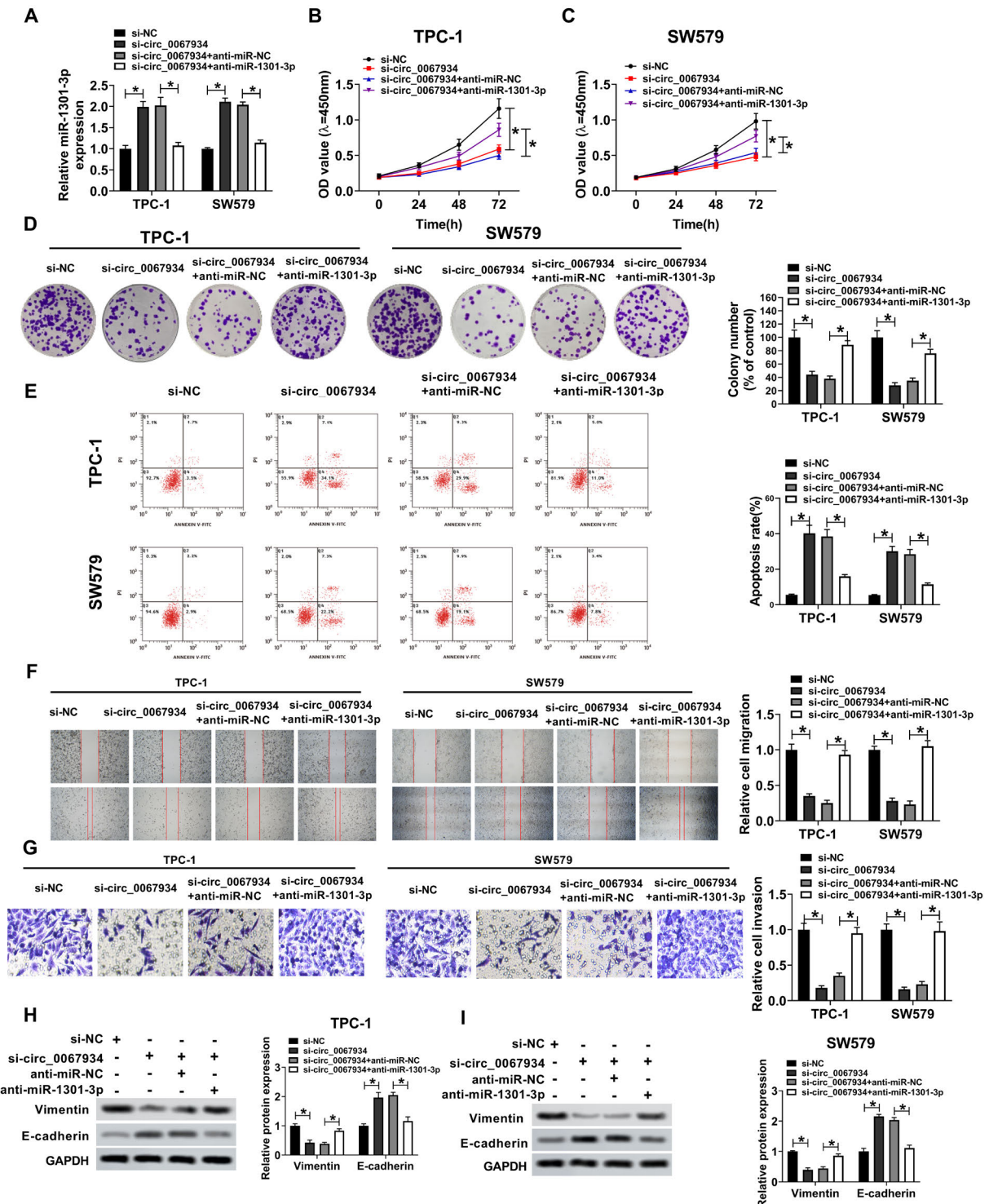


Figure 4. Depletion of miR-1301-3p suppresses the effects of circ_00067934 knockdown in PTC cells. TPC-1 and SW579 cells were transfected with si-NC, si-circ_00067934, anti-miR-NC, or anti-miR-1301-3p as indicated in the following experiments. (A) The expression of miR-1301-3p in TPC-1 and SW579 cells was tested by qRT-PCR. (B and C) TPC-1 and SW579 cells were seeded in 96-well plates (3000 cells/well), then cell viability at 0, 24, 48, and 72 h was evaluated. (D) TPC-1 and SW579 cells were seeded in 6-well plates (500 cells/well) for colony formation assay. Representative plates and colony numbers are shown. (E) TPC-1 and SW579 cells were used for flow cytometry analysis. (F) TPC-1 and SW579 cells were used for the wound-healing assay. Representative images and relative migration distance are shown. (G) TPC-1 and SW579 cells were used for the Transwell invasion assay. Representative images and relative invasion cells are shown. (H and I) TPC-1 and SW579 cells were used for western blot. * $p < 0.05$. Each sample was done in triplicate.

the underlying molecular mechanism of circ_0067934 in PTC (Supplementary Figure S3).

Discussion

Numerous studies indicate that circ_0067934 is involved in tumorigenesis and progression of many cancers. For example, upregulation of circ_0067934 is associated with tumor growth and poor prognosis of non-small cell lung cancer (NSCLC) patients [36], and silencing of circ_0067934 inhibits proliferation, migration, and invasion of NSCLC cells [37]. The cancer promotion effects of circ_0067934 are also

observed in esophageal squamous cell carcinoma, bladder cancer, and cervical cancer [24, 25, 38]. More importantly, Wang et al. find that circ_0067934 is upregulated and correlated poor prognosis of TC [26]. This study also suggests that circ_0067934 inhibits proliferation, migration, invasion, EMT, and induces apoptosis of TC cells by regulating the PI3K/Akt signaling. However, the underlying molecular mechanism of circ_0067934 in TC is not fully elucidated by this study. Besides, Zhang et al. reported that circ_0067934 knockdown suppressed proliferation, migration, invasion, and tumor growth and promoted apoptosis of TC cells through the miR-1304/CXCR1 axis [22]. In our study, we also

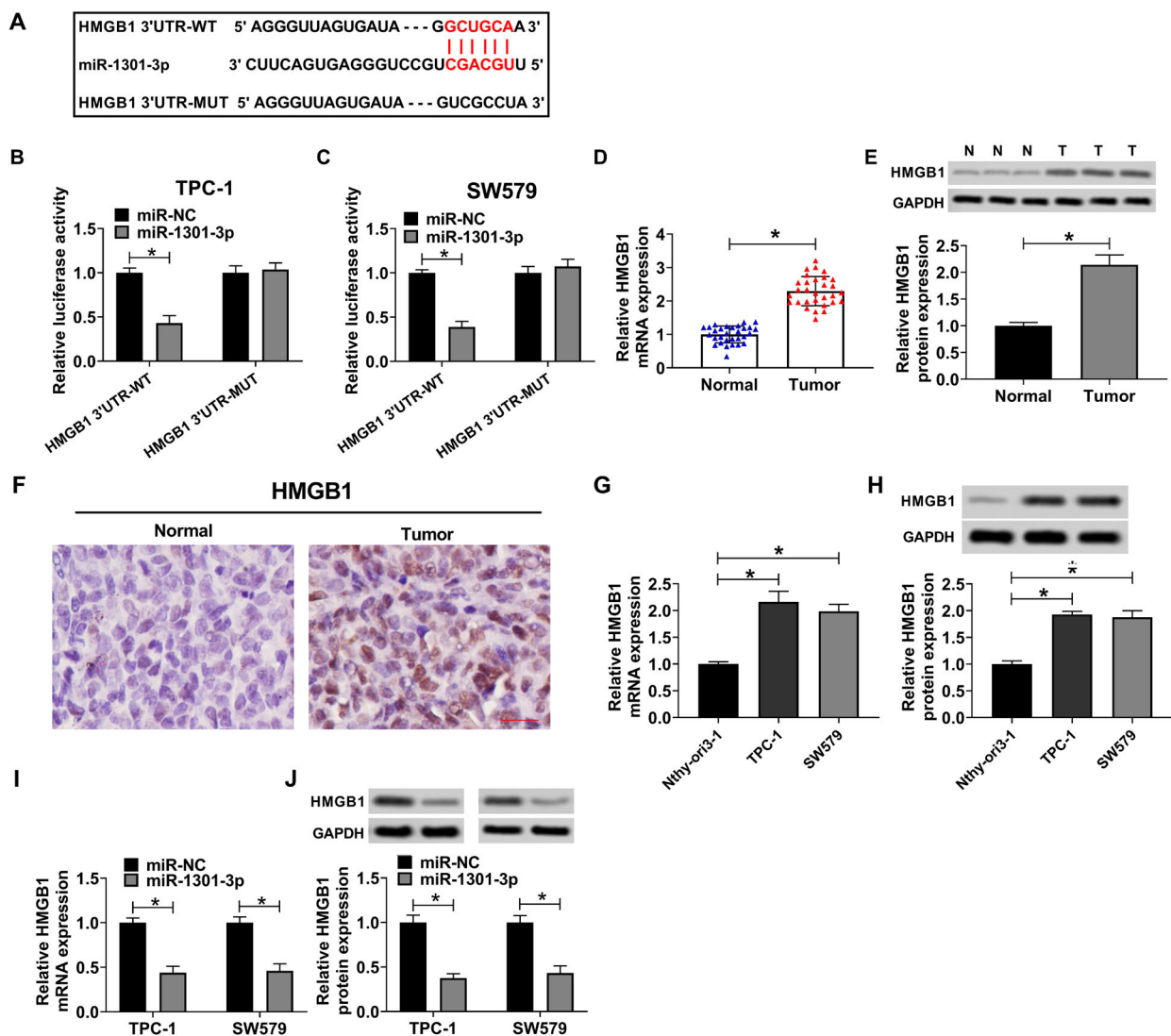


Figure 5. HMGB1 is a target of miR-1301-3p in PTC cells. (A) The predicted binding sites of HMGB1 and miR-1301-3p. (B and C) TPC-1 and SW579 cells were co-transfected with HMGB1 WT or MUT, miR-1301-3p, or miR-NC for the luciferase reporter assay. (D–F) The mRNA and protein expression of HMGB1 in PTC samples and matched normal tissues were evaluated by qRT-PCR, western blot, and IHC staining. Scale bar = 50 μ m. (G and H) The level of HMGB1 in Nthy-ori3-1, TPC-1, and SW579 cells was measured by qRT-PCR and western blot. (I and J) TPC-1 and SW579 cells were transfected with miR-NC and miR-1301-3p, then the level of HMGB1 was measured by qRT-PCR and western blot. * $p < 0.05$. Each sample was done in triplicate.

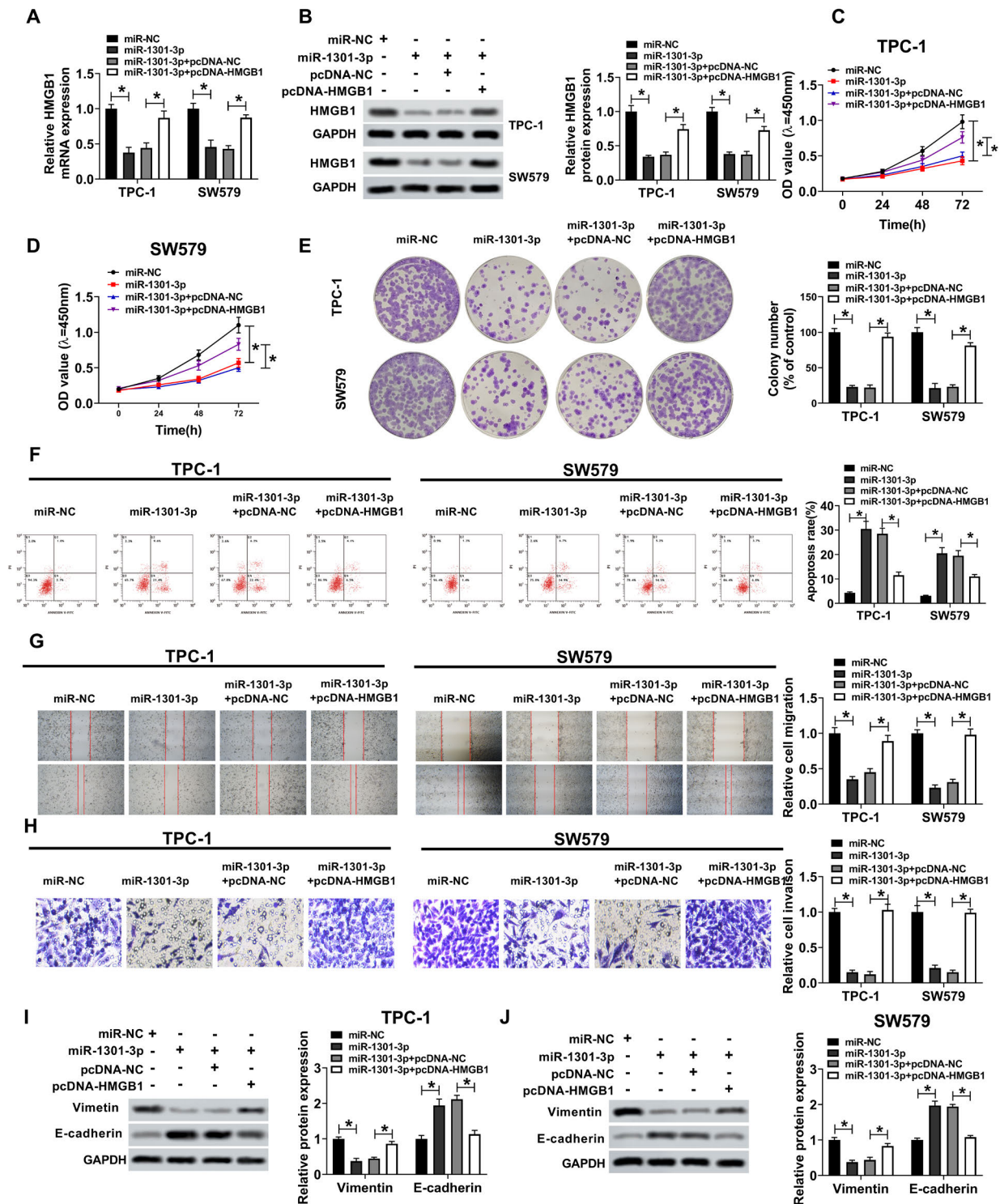


Figure 6. miR-1301-3p inhibits the malignant potential of PTC cells via suppressing HMGB1. TPC-1 and SW579 cells were transfected with miR-NC, miR-1301-3p, pcDNA-NC, or pcDNA-HMGB1 as indicated for the following experiments. (A and B) The mRNA and protein expression of HMGB1 in TPC-1 and SW579 cells were tested by qRT-PCR and western blot assay. (C and D) TPC-1 and SW579 cells were seeded in 96-well plates (3000 cells/well), then cell viability at 0, 24, 48, and 72 h was evaluated. (E) TPC-1 and SW579 cells were seeded in 6-well plates (500 cells/well) for colony formation assay. Representative plates and colony numbers are shown. (F) TPC-1 and SW579 cells were used for the flow cytometry analysis. (G) TPC-1 and SW579 cells were used for the wound-healing assay. Representative images and relative migration distance are shown. (H) TPC-1 and SW579 cells were used for the Transwell invasion assay. Representative images and relative invasion cells were shown. (I and J) TPC-1 and SW579 cells were used for western blot. * $p < 0.05$. Each sample was done in triplicate.

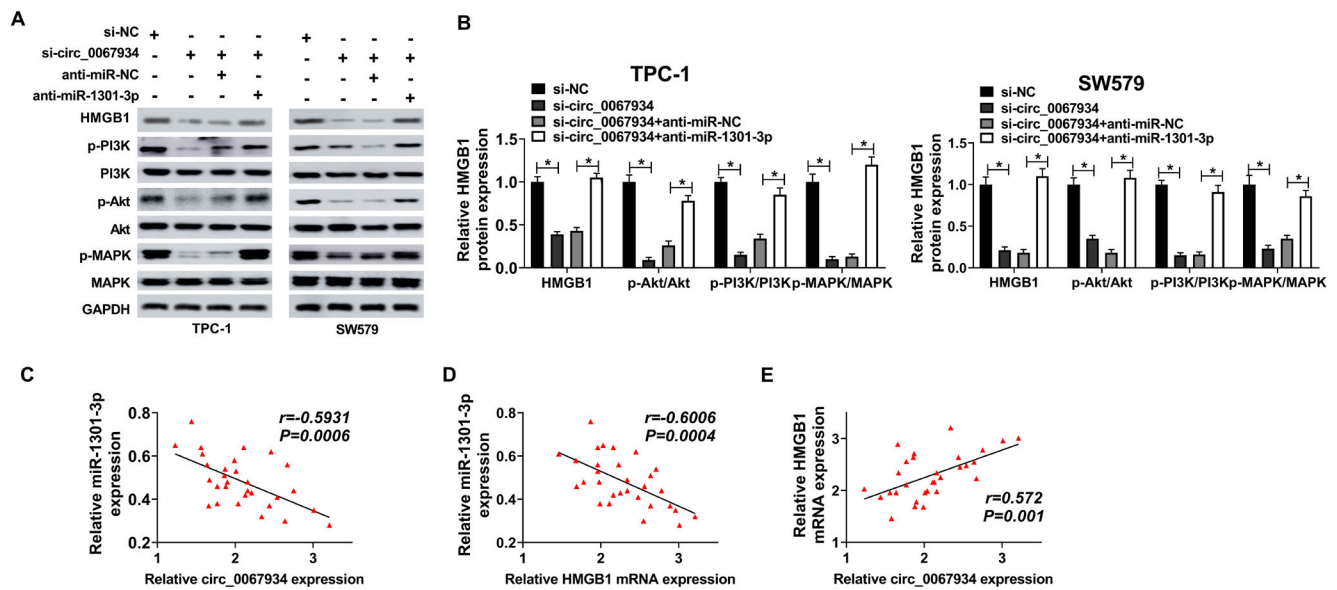


Figure 7. Knockdown of circ_0067934 suppressed HMGB1 expression, PI3K/Akt and MAPK activation through sponging miR-1301-3p. **A, B)** TPC-1 and SW579 cells were transfected with si-NC, si-circ_0067934, anti-miR-NC, or anti-miR-1301-3p as indicated, then collected lysates for western blot assay. **(C)** The Pearson correlation of miR-1301-3p and circ_0067934 expression in 30 thyroid cancer patients. **(D)** The Pearson correlation of miR-1301-3p and HMGB1 expression in 30 thyroid cancer patients. **(E)** The Pearson correlation of HMGB1 and circ_0067934 expression in 30 thyroid cancer patients. * $p < 0.05$.

found that silencing circ_0067934 inhibited proliferation, migration, invasion, and EMT of PTC cells, corresponding with previous studies. Moreover, we demonstrated that circ_0067934 overexpression promoted anchorage-independent growth of normal thyroid cell Nthy-ori3-1, suggesting that circ_0067934 played an oncogenic role in PTC. In addition, we found that silencing circ_0067934 suppressed colony formation of PTC cells. These effects of circ_0067934 might due to regulating the miR-1301-3p/HMGB1 axis and subsequently mediating PI3K/Akt and MAPK activation in PTC cells. This was different from Zhang's report, and we reasoned that circ_0067934 might act as a molecular sponge for not only one miRNA in TC but for more miRNAs. Indeed, circ_0067934 is reported to sponge several other miRNAs such as miR-1182 in NSCLC [31], miR-1304 in bladder cancer and TC [22, 38], and miR-545 in cervical cancer [25]. Though these previous studies reduced the novelty of our study, we provided a clear elucidation and novel insight into the function of circ_0067934 in the progression of PTC cells. Our study also provided a novel molecular mechanism of circ_0067934 in PTC cells.

It is widely acknowledged that circRNA-miRNA-mRNA interactions play a key role in the tumorigenesis of cancers. In our study, miR-1301-3p was predicted to be a direct target of circ_0067934, and our results demonstrated that circ_0067934 acted as a molecular sponge for miR-1301-3p in PTC cells. Moreover, we found that depletion of miR-1301-3p suppresses the effects of circ_0067934 knock-down in PTC cells. We focused on miR-1301-3p in our study

because previous studies indicated that miR-1301-3p was downregulated and acted as a tumor suppressor in PTC [39]. The tumor suppressor role of miR-1301-3p in cancers has been well-characterized. For example, miR-1301 is proved to suppress migration and invasion of multiple human cancer cells by regulating the p53/UBE4B axis [40]. In breast cancer, miR-1301-3p is downregulated and inhibits the proliferation of breast cancer cells by directly targeting ICT1 [41]. In PTC, Qiao et al. proved that miR-1301-3p is decreased in PTC patients and cell lines, and enforced miR-1301-3p expression suppresses proliferation of PTC cells [39]. In our study, we also found that miR-1301-3p was downregulated in PTC patients, and we speculated that miR-1301-3p might be a prognostic marker for PTC, too. Virtually, the function of miR-1301-3p in PTC is also reported by another study. Wen et al. report that miR-1301-3p is sponged by lncRNA ABHD11-AS1 thus promoting PTC progression by regulating the PI3K/Akt pathway [42]. These studies and our results pointed out a critical role of miR-1301-3p in tumorigenesis and progression of PTC, and miR-1301-3p might be a therapeutic target for PTC treatment.

HMGB1 is a ubiquitous chromatin component of mammalian cells that regulates gene transcription. HMGB1 overexpression has been observed in a variety of human cancers. In our study, we found that HMGB1 was a downstream target of miR-1301-3p. HMGB1 expression was significantly upregulated in PTC specimens. Moreover, we proved that miR-1301-3p inhibited the malignant potential of PTC cells via suppressing HMGB1. We focused on HMGB1 in our

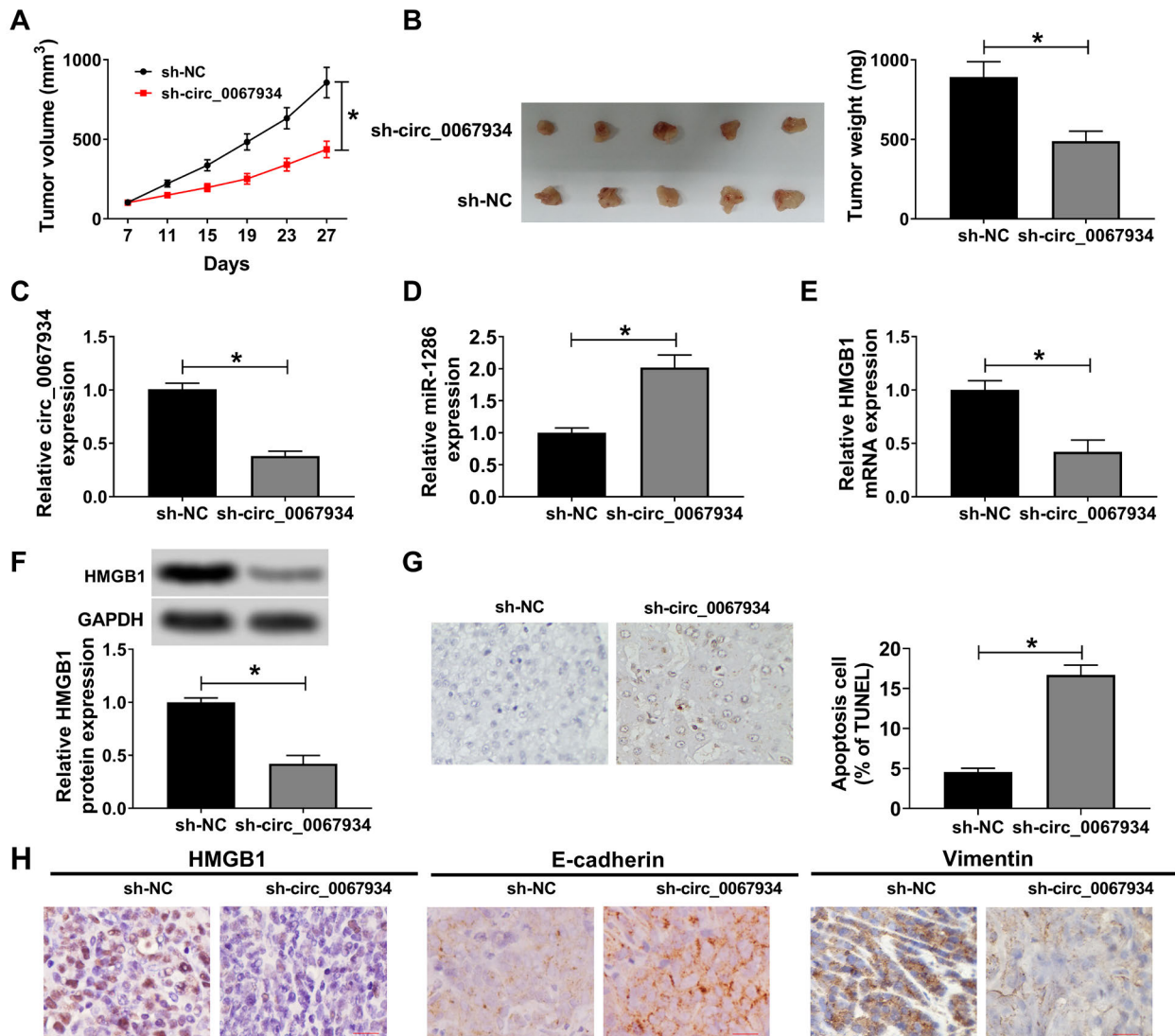


Figure 8. circ_0067934 depletion repressed tumor xenograft growth of PTC cells. (A and B) TPC-1 cells (4×10^6) stably transfected with sh-circ_0067934 or sh-NC were subcutaneously injected into nude mice, then tumor growth, tumor volume, and weight were evaluated. (C-E) The levels of circ_0067934, miR-1301-3p, and HMGB1 in tumor xenografts were evaluated by qRT-PCR. (F) The protein expression of HMGB1 in tumor xenografts was evaluated by western blot. (G) TUNEL staining was used to detect cell apoptosis in tumor xenografts. (H) Expressions of HMGB1, E-cadherin, and vimentin were observed by IHC staining in tumor xenografts of mouse model. * $p < 0.05$. Each sample was done in triplicate.

study because accumulated studies pointed to an important role of HMGB1 in the initiation and progression of PTC. For example, HMGB1 is proved to upregulate and facilitate the growth and motility of PTC cells by inducing miR-222 and miR-221 expression [43]. Besides, upregulation of HMGB1 is associated with NF- κ B activation and inflammatory infiltrates of PTC [44]. Ding et al. found that knockdown of HMGB1 inhibits proliferation, migration, and invasion in PTC cells [45]. Ye et al. found that HMGB1 is involved in circFOXM1 mediated regulation of tumor growth of PTC cells *in vitro* and *in vivo* [30]. These studies and our results revealed a cancer-promoting role of HMGB1 in PTC development and

HMGB1 might be a prognostic marker or therapeutic target for PTC treatment. In addition, our results indicated that knockdown of circ_0067934 suppressed HMGB1 expression, PI3K/Akt and MAPK activation through sponging miR-1301-3p. Indeed, HMGB1 is demonstrated to regulate multiple signaling pathways including PI3K/Akt and MAPK. For example, HMGB1 overexpression induces miR-221/222 expression, thus, in turn, reducing PTEN expression (a negative regulator for the PI3K/Akt signaling) in PTC cells [46]. In prostate cancer, HMGB1 promotes proliferation and metastasis of prostate cancer cells by activating the Akt signaling [34]. In breast cancer, HMGB1 enhances vessel

formation and invasion of breast cancer cells via regulating the PI3K/Akt signaling [47]. HMGB1 is also reported to regulate MAPK signaling in human bronchial epithelial cells [48], mesenchymal stem cells [49], and hepatocellular carcinoma cells [50].

There are potential limitations of our study. As circ_0067934 can be a molecular sponge for multiple miRNAs, and miR-1301-3p may have multiple targets in PTC cells, we cannot rule out the possibility of another signaling axis that is involved in the functions of circ_0067934 in PTC. Moreover, most of our experiments are in cultured cell lines and nude mice, these results may be different in human subjects and more studies are needed to confirm this. Finally, as the function of circ_0067934 in PTC has been reported by others, the novelty of our study might decrease. However, we gave a full elucidation of the function of circ_0067934 in PTC cells *in vitro* and *in vivo*, and novel functions and new underlying molecular mechanism of circ_0067934 are discovered in our study.

In summary, we found that circ_0067934 was upregulated in PTC tissues and cell lines. Silencing circ_0067934 suppressed growth, colony formation, migration, invasion, EMT, and tumor xenograft growth of PTC cells *in vitro* and *in vivo*. Moreover, circ_0067934 acted as a molecular sponge for miR-1301-3p, thus regulating HMGB1 expression, PI3K/Akt and MAPK signaling in PTC cells. Our results provided a novel insight into circ_0067934 in the tumorigenesis and progression of PTC. circ_0067934 might be a prognostic marker or therapeutic target for PTC treatment.

Supplementary information is available in the online version of the paper.

Acknowledgments: This study was supported by the Henan Province Medical Science and Technology Research Project (LHGJ20190447).

References

- [1] SIEGEL RL, MILLER KD, JEMAL A. Cancer statistics, 2020. *CA Cancer J Clin* 2020; 70: 7–30. <https://doi.org/10.3322/caac.21590>
- [2] CARLING T, UDELSMAN R. Thyroid Cancer. *Annu Rev Med* 2014; 65: 125–137. <https://doi.org/10.1146/annurev-med-061512-105739>
- [3] RANGEL-POZZO A, SISDELLI L, CORDIOLI MIV, VASISMAN F, CARIA P et al. Genetic Landscape of Papillary Thyroid Carcinoma and Nuclear Architecture: An Overview Comparing Pediatric and Adult Populations. *Cancers (Basel)* 2020; 12: 3146. <https://doi.org/10.3390/cancers12113146>
- [4] YE M, HOU H, SHEN M, DONG S, ZHANG T. Circular RNA circFOXO1 Plays a Role in Papillary Thyroid Carcinoma by Sponging miR-1179 and Regulating HMGB1 Expression. *Mol Ther Nucleic Acids* 2019; 19: 741–750. <https://doi.org/10.1016/j.omtn.2019.12.014>
- [5] BLOMBERG M, FELDT-RASMUSSEN U, ANDERSEN KK, KJAER SK. Thyroid cancer in Denmark 1943–2008, before and after iodine supplementation. *Int J Cancer* 2012; 131: 2360–2366. <https://doi.org/10.1002/ijc.27497>
- [6] MUHAMMAD N, STEELE R, ISBELL TS, PHILIPS N, RAY RB. Bitter melon extract inhibits breast cancer growth in pre-clinical model by inducing autophagic cell death. *Oncotarget* 2017; 8: 66226–66236. <https://doi.org/10.18632/oncotarget.19887>
- [7] MOHAMMAD N, MALVI P, MEENA AS, SINGH SV, CHAUBE B et al. Cholesterol depletion by methyl- β -cyclodextrin augments tamoxifen induced cell death by enhancing its uptake in melanoma. *Mol Cancer* 2014; 13: 204. <https://doi.org/10.1186/1476-4598-13-204>
- [8] MOHAMMAD N, SINGH SV, MALVI P, CHAUBE B, ATHAVALE D et al. Strategy to enhance efficacy of doxorubicin in solid tumor cells by methyl- β -cyclodextrin: Involvement of p53 and Fas receptor ligand complex. *Sci Rep* 2015; 5: 11853. <https://doi.org/10.1038/srep11853>
- [9] RASHMI R, JAYACHANDRAN K, ZHANG J, MENON V, MUHAMMAD N et al. Glutaminase Inhibitors Induce Thiol-Mediated Oxidative Stress and Radiosensitization in Treatment-Resistant Cervical Cancers. *Mol Cancer Ther* 2020; 19: 2465–2475. <https://doi.org/10.1158/1535-7163.MCT-20-0271>
- [10] FEDERICO C, SUN J, MUZ B, ALHALLAK K, COSPER PF et al. Localized Delivery of Cisplatin to Cervical Cancer Improves Its Therapeutic Efficacy and Minimizes Its Side Effect Profile. *Int J Radiat Oncol Biol Phys* 2021; 109: 1483–1494. <https://doi.org/10.1016/j.ijrobp.2020.11.052>
- [11] MUHAMMAD N, BHATTACHARYA S, STEELE R, PHILIPS N, RAY RB. Involvement of c-Fos in the Promotion of Cancer Stem-like Cell Properties in Head and Neck Squamous Cell Carcinoma. *Clin Cancer Res* 2017; 23: 3120–3128. <https://doi.org/10.1158/1078-0432.CCR-16-2811>
- [12] KUMAR B, CHAND V, RAM A, USMANI D, MUHAMMAD N. Oncogenic Mutations in Tumorigenesis and Targeted Therapy in Breast Cancer. *Curr Mol Bio Rep* 2020; 6: 116–125. <https://doi.org/10.1007/s40610-020-00136-x>
- [13] ELGUINDY MM, MENDELL JT. NORAD-induced Pumi-lio phase separation is required for genome stability. *Nature* 2021; 595: 303–308. <https://doi.org/10.1038/s41586-021-03633-w>
- [14] MAO C, WANG X, LIU Y, WANG M, YAN B et al. A G3BP1-Interacting lncRNA Promotes Ferroptosis and Apoptosis in Cancer via Nuclear Sequestration of p53. *Cancer Res* 2018; 78: 3484–3496. <https://doi.org/10.1158/0008-5472.CAN-17-3454>
- [15] WANG M, MAO C, OUYANG L, LIU Y, LAI W et al. Long noncoding RNA LINC00336 inhibits ferroptosis in lung cancer by functioning as a competing endogenous RNA. *Cell Death Differ* 2019; 26: 2329–2343. <https://doi.org/10.1038/s41418-019-0304-y>
- [16] LI D Y, BUSCH A, JIN H, CHERNOGUBOVA E, PELISEK J et al. H19 Induces Abdominal Aortic Aneurysm Development and Progression. *Circulation* 2018; 138: 1551–1568. <https://doi.org/10.1161/CIRCULATIONAHA.117.032184>

- [17] MONTES M, LUBAS M, ARENDRUP FS, MENTZ B, ROHATGI N et al. The long non-coding RNA MIR31HG regulates the senescence associated secretory phenotype. *Nat Commun* 2021; 12: 2459. <https://doi.org/10.1038/s41467-021-22746-4>
- [18] YANG R, LIU N, CHEN L, JIANG Y, SHI Y et al. GIAT4RA functions as a tumor suppressor in non-small cell lung cancer by counteracting Uchl3-mediated deubiquitination of LSH. *Oncogene* 2019; 38: 7133–7145. <https://doi.org/10.1038/s41388-019-0909-0>
- [19] CHIEN Y, TSAI PH, LAI YH, LU KH, LIU CY et al. CircularRNA as novel biomarkers in liver diseases. *J Chin Med Assoc* 2020; 83: 15–17. <https://doi.org/10.1097/JCMA.000000000000230>
- [20] BI W, HUANG J, NIE C, LIU B, HE G et al. CircRNA circRNA_102171 promotes papillary thyroid cancer progression through modulating CTNNBIP1-dependent activation of beta-catenin pathway. *J Exp Clin Cancer Res* 2018; 37: 275. <https://doi.org/10.1186/s13046-018-0936-7>
- [21] YAO Y, CHEN X, YANG H, CHEN W, QIAN Y et al. Hsa_circ_0058124 promotes papillary thyroid cancer tumorigenesis and invasiveness through the NOTCH3/GATAD2A axis. *J Exp Clin Cancer Res* 2019; 38: 318. <https://doi.org/10.1186/s13046-019-1321-x>
- [22] ZHANG H, MA X P, LI X, DENG F S. Circular RNA circ_0067934 exhaustion expedites cell apoptosis and represses cell proliferation, migration and invasion in thyroid cancer via sponging miR-1304 and regulating CXCR1 expression. *Eur Rev Med Pharmacol Sci* 2019; 23: 10851–10866. https://doi.org/10.26355/eurrev_201912_19789
- [23] ZHU Q, LU G, LUO Z, GUI F, WU J et al. CircRNA circ_0067934 promotes tumor growth and metastasis in hepatocellular carcinoma through regulation of miR-1324/FZD5/Wnt/beta-catenin axis. *Biochem Biophys Res Commun* 2018; 497: 626–632. <https://doi.org/10.1016/j.bbrc.2018.02.119>
- [24] XIA W, QIU M, CHEN R, WANG S, LENG X et al. Circular RNA has_circ_0067934 is upregulated in esophageal squamous cell carcinoma and promoted proliferation. *Sci Rep* 2016; 6: 35576. <https://doi.org/10.1038/srep35576>
- [25] HU C, WANG Y, LI A, ZHANG J, XUE F et al. Overexpressed circ_0067934 acts as an oncogene to facilitate cervical cancer progression via the miR-545/EIF3C axis. *J Cell Physiol* 2019; 234: 9225–9232. <https://doi.org/10.1002/jcp.27601>
- [26] WANG H, YAN X, ZHANG H, ZHAN X. CircRNA circ_0067934 Overexpression Correlates with Poor Prognosis and Promotes Thyroid Carcinoma Progression. *Med Sci Monit* 2019; 25: 1342–1349. <https://doi.org/10.12659/MSM.913463>
- [27] MUHAMMAD N, BHATTACHARYA S, STEELE R, RAY RB. Anti-miR-203 suppresses ER-positive breast cancer growth and stemness by targeting SOCS3. *Oncotarget* 2016; 7: 58595–58605. <https://doi.org/10.18632/oncotarget.11193>
- [28] HAN M, WANG S, FRITAH S, WANG X, ZHOU W et al. Interfering with long non-coding RNA MIR22HG processing inhibits glioblastoma progression through suppression of Wnt/beta-catenin signalling. *Brain* 2020; 143: 512–530. <https://doi.org/10.1093/brain/awz406>
- [29] CHEN Q, LIU T, BAO Y, ZHAO T, WANG J et al. CircRNA cRAPGEF5 inhibits the growth and metastasis of renal cell carcinoma via the miR-27a-3p/TXNIP pathway. *Cancer Lett* 2020; 469: 68–77. <https://doi.org/10.1016/j.canlet.2019.10.017>
- [30] YE M, HOU H, SHEN M, DONG S, ZHANG T. Circular RNA circFOXM1 Plays a Role in Papillary Thyroid Carcinoma by Sponging miR-1179 and Regulating HMGB1 Expression. *Mol Ther Nucleic Acids* 2020; 19: 741–750. <https://doi.org/10.1016/j.omtn.2019.12.014>
- [31] ZHAO M, MA W, MA C. Circ_0067934 promotes non-small cell lung cancer development by regulating miR-1182/KLF8 axis and activating Wnt/beta-catenin pathway. *Biomed Pharmacother* 2020; 129: 110461. <https://doi.org/10.1016/j.biopha.2020.110461>
- [32] BOROWICZ S, VAN SCOYK M, AVASARALA S, KARUPPUSAMY RATHINAM MK, TAULER J et al. The soft agar colony formation assay. *J Vis Exp* 2014; 92: e51998. <https://doi.org/10.3791/51998>
- [33] LI R, ZOU X, HUANG H, YU Y, ZHANG H et al. HMGB1/PI3K/Akt/mTOR Signaling Participates in the Pathological Process of Acute Lung Injury by Regulating the Maturation and Function of Dendritic Cells. *Front Immunol* 2020; 11: 1104. <https://doi.org/10.3389/fimmu.2020.01104>
- [34] LV DJ, SONG XL, HUANG B, YU YZ, SHU FP et al. HMGB1 Promotes Prostate Cancer Development and Metastasis by Interacting with Brahma-Related Gene 1 and Activating the Akt Signaling Pathway. *Theranostics* 2019; 9: 5166–5182. <https://doi.org/10.7150/thno.33972>
- [35] XIE W, ZHU T, DONG X, NAN F, MENG X et al. HMGB1-triggered inflammation inhibition of notoginseng leaf triterpenes against cerebral ischemia and reperfusion injury via MAPK and NF-kappaB signaling pathways. *Biomolecules* 2019; 9: 512. <https://doi.org/10.3390/biom9100512>
- [36] ZOU Q, WANG T, LI B, LI G, ZHANG L et al. Overexpression of circ-0067934 is associated with increased cellular proliferation and the prognosis of non-small cell lung cancer. *Oncol Lett* 2018; 16: 5551–5556. <https://doi.org/10.3892/ol.2018.9357>
- [37] WANG J, LI H. CircRNA circ_0067934 silencing inhibits the proliferation, migration and invasion of NSCLC cells and correlates with unfavorable prognosis in NSCLC. *Eur Rev Med Pharmacol Sci* 2018; 22: 3053–3060. https://doi.org/10.26355/eurrev_201805_15063
- [38] LIU Q, ZHOU Q, ZHONG P. circ_0067934 increases bladder cancer cell proliferation, migration and invasion through suppressing miR-1304 expression and increasing Myc expression levels. *Exp Ther Med* 2020; 19: 3751–3759. <https://doi.org/10.3892/etm.2020.8648>
- [39] QIAO DH, HE XM, YANG H, ZHOU Y, DENG X et al. miR-1301-3p suppresses tumor growth by downregulating PCNA in thyroid papillary cancer. *Am J Otolaryngol* 2021; 42: 102920. <https://doi.org/10.1016/j.amjoto.2021.102920>
- [40] WANG B, WU H, CHAI C, LEWIS J, PICHIORRI F et al. MicroRNA-1301 suppresses tumor cell migration and invasion by targeting the p53/UBE4B pathway in multiple human cancer cells. *Cancer Lett* 2017; 401: 20–32. <https://doi.org/10.1016/j.canlet.2017.04.038>

- [41] PENG X, YAN B, SHEN Y. MiR-1301-3p inhibits human breast cancer cell proliferation by regulating cell cycle progression and apoptosis through directly targeting ICT1. *Breast Cancer* 2018; 25: 742–752. <https://doi.org/10.1007/s12282-018-0881-5>
- [42] WEN J, WANG H, DONG T, GAN P, FANG H et al. STAT3-induced upregulation of lncRNA ABHD11-AS1 promotes tumour progression in papillary thyroid carcinoma by regulating miR-1301-3p/STAT3 axis and PI3K/AKT signalling pathway. *Cell Prolif* 2019; 52: e12569. <https://doi.org/10.1111/cpr.12569>
- [43] MARDENTE S, MARI E, CONSORTI F, DI GIOIA C, NEGRI R et al. HMGB1 induces the overexpression of miR-222 and miR-221 and increases growth and motility in papillary thyroid cancer cells. *Oncol Rep* 2012; 28: 2285–2289. <https://doi.org/10.3892/or.2012.2058>
- [44] MARDENTE S, ZICARI A, CONSORTI F, MARI E, DI VITO M et al. Cross-talk between NO and HMGB1 in lymphocytic thyroiditis and papillary thyroid cancer. *Oncol Rep* 2010; 24: 1455–1461. https://doi.org/10.3892/or_00001005
- [45] DING C, YU H, SHI C, SHI T, QIN H et al. MiR-let-7e inhibits invasion and migration and regulates HMGB1 expression in papillary thyroid carcinoma. *Biomed Pharmacother* 2019; 110: 528–536. <https://doi.org/10.1016/j.biopha.2018.11.057>
- [46] MARDENTE S, MARI E, MASSIMI I, FICO F, FAGGIONI A et al. HMGB1-Induced Cross Talk between PTEN and miRs 221/222 in Thyroid Cancer. *Biomed Res Int* 2015; 2015: 512027. <https://doi.org/10.1155/2015/512027>
- [47] HE H, WANG X, CHEN J, SUN L, SUN H et al. High-Mobility Group Box 1 (HMGB1) Promotes Angiogenesis and Tumor Migration by Regulating Hypoxia-Inducible Factor 1 (HIF-1alpha) Expression via the Phosphatidylinositol 3-Kinase (PI3K)/AKT Signaling Pathway in Breast Cancer Cells. *Med Sci Monit* 2019; 25: 2352–2360. <https://doi.org/10.12659/MSM.915690>
- [48] LIANG Y, HOU C, KONG J, WEN H, ZHENG X et al. HMGB1 binding to receptor for advanced glycation end products enhances inflammatory responses of human bronchial epithelial cells by activating p38 MAPK and ERK1/2. *Mol Cell Biochem* 2015; 405: 63–71. <https://doi.org/10.1007/s11010-015-2396-0>
- [49] FENG L, XUE D, CHEN E, ZHANG W, GAO X et al. HMGB1 promotes the secretion of multiple cytokines and potentiates the osteogenic differentiation of mesenchymal stem cells through the Ras/MAPK signaling pathway. *Exp Ther Med* 2016; 12: 3941–3947. <https://doi.org/10.3892/etm.2016.3857>
- [50] CHEN Y, LIN C, LIU Y, JIANG Y. HMGB1 promotes HCC progression partly by downregulating p21 via ERK/c-Myc pathway and upregulating MMP-2. *Tumour Biol* 2016; 37: 4399–4408. <https://doi.org/10.1007/s13277-015-4049-z>